JMEPEG (2021) 30:1066–1074
https://doi.org/10.1007/s11665-020-05445-x

1059-9495/$19.00

Effect of Heat Treatment Procedure on Mechanical Properties of Ti-15V-3Al-3Sn-3Cr Metastable β Titanium Alloy

Nihal Yumak and Kubilay Aslantaş

Submitted: 31 August 2020 / Revised: 23 November 2020 / Accepted: 1 December 2020 / Published online: 8 January 2021

In this study, the effects of various heat treatment procedures on the mechanical properties of the Ti-15V-3Al-3Sn-3Cr metastable β titanium alloy were investigated. Single-step and duplex aging treatments were applied to the alloy at low and high aging temperatures. Duplex aging treatments were carried out by selecting two different pre-aging times and temperatures: 10 h at 300 °C and 24 h at 250 °C. Thus, the effects of pre-aging on the mechanical properties of the alloy were examined. Optimum tensile properties were obtained in the duplex-aged samples, which was aged at 550 °C for 20 h after being pre-aged at 250 °C for 24 h. While fine, high volume fraction and uniformly dispersed α phases increased the tensile strength and % elongation of the alloy in the aging treatment, the fatigue crack propagation rate also increased. Also, it was observed that the threshold stress intensity factor range (ΔK_{th}) increased with the aging treatment. While the lowest ΔK_{th} value was obtained at the solution-treated sample, the highest ΔK_{th} value was obtained in the sample to which duplex aging treatment was applied depending on precipitation of fine and high volume fraction of α phases.

Keywords aging treatment, fatigue crack propagation rate, mechanical properties, metastable β titanium alloys, threshold stress intensity factor range, Ti-15V-3Al-3Sn-3Cr alloy

1. Introduction

The properties expected from materials used in the aerospace, space and biomedical fields are high tensile strength, low density, high fatigue strength and good formability (Ref 1). The use of metastable β titanium alloys has become widespread in the last 10 years since it can provide all these properties together (Ref 2). The Ti-15V-3Al-3Sn-3Cr alloy, which is one of the metastable β titanium alloys, has been developed as an alternative to the Ti-10V-2Fe-3Al alloy in order to meet the thin sheet material requirement in aerospace applications (Ref 3). The Ti-15V-3Al-3Sn-3Cr metastable β phase titanium alloys can be heat-treated efficiently thanks to its low molybdenum equivalent (11) (Ref 4). In the study conducted by Qiang et al., the tensile strength of the Ti-15V-3Al-3Sn-3Cr alloy (799 MPa) was found to be 1562 MPa after cold rolling and aging treatment at 450 °C for 4 h (Ref 5).

Precipitation hardening is the primary heat treatment applied to metastable β titanium alloys. Precipitation hardening consists of two stages, including the solution treatment and aging treatment. The solution treatment can be applied in the α/β region below the beta transition temperature (T_β), or in the β region at temperatures above the T_β (Ref 4). The solution treatment temperature determines the mechanical properties of the alloy by affecting the grain size and the stability of the β phases (Ref 6). When the alloy is solutionized in the α/β region, the primary α phases precipitate at β grain boundaries, thereby preventing recrystallization and grain formation, so achieving a smaller grain size (Ref 7). Although it is thought that solutionization in the α/β region may increase the mechanical properties by reducing the grain size, the aging treatment efficiency decreases by increasing the β phase stability (Ref 8).

In the literature, it has been observed that aging treatments applied to metastable β titanium alloys are generally applied as either single step or duplex (Ref 9, 10). Single-step aging treatments can be applied in two different temperature groups: low and high temperatures, in terms of precipitation order and α phase formation morphology (Ref 8, 11). Low-temperature aging treatment is applied between 200 and 450 °C, and high-temperature aging treatment is applied at temperatures of 85-195 °C below T_β (550-700 °C) and for less than 24 h (Ref 12). While isothermal ω_{iso} metastable phases are formed earlier than α phases at low temperatures, these phases cannot occur due to the increase in precipitation kinetics at high temperatures (Ref 13). Duplex aging treatments are performed gradually by applying short-term high-temperature second-step aging treatment after low-temperature pre-aging treatment (Ref 13, 14). During the pre-aging treatment, ω_{iso}/β interfaces are formed in which α phases are precipitated in the second-step aging treatment (Ref 14). This increases the tensile strength and high cycle fatigue life of metastable β titanium alloys by providing fine, uniformly distributed and high volume fraction α phases, and reducing precipitation free zones [13, 15).

Metastable β titanium alloys are frequently exposed to fatigue damage in the landing gear system and fasteners used in aerospace applications (Ref 16). Therefore, it is important to investigate the fatigue behavior of metastable β titanium alloys. In the literature review on this subject, several studies investigating the effect of precipitation hardening on high

Nihal Yumak and **Kubilay Aslantaş**, Department of Mechanical Engineering, Afyon Kocatepe University, Afyonkarahisar, Turkey. Contact e-mails: nyumak@aku.edu.tr and aslantas@aku.edu.tr.

cycle fatigue behavior of metastable β titanium alloys were found (Ref 13, 17). In these studies, especially with the application of the duplex aging treatment, the reduction of the precipitation free zones and the fine uniform precipitation of the α phases increased the high cycle fatigue strength (Ref 13).

In the literature review (Ref 9, 15), many studies were found in which microstructural and mechanical properties of metastable β titanium alloys were investigated by applying various heat treatments. However, these studies were found to be insufficient to understand the effect of single-step and duplex aging treatments on the tensile properties and fatigue crack propagation behavior of metastable β titanium alloys. For this reason, it is aimed to investigate in detail the effect of single-step and duplex aging treatments on the mechanical and microstructural properties of the alloy by applying aging treatment in all temperature and time groups. In addition, by applying fatigue crack propagation test to each sample group, the effect of aging treatments on fatigue crack growth and propagation behavior of the alloy will be determined.

2. Materials and Methods

Ti-15V-3Al-3Sn-3Cr alloy was supplied by Baoji Litail from China. The chemical composition of the alloy was given as follows in accordance with the test certificate received from Baoji Litail: V = 15.79 (wt.%), Al = 2.74 (wt.%), Sn = 3.03 (wt.%), Cr = 3.12 (wt.%), Fe = 0.008 (wt.%), C = 0.01 (wt.%), N = 0.008 (wt.%), O = 0.096 (wt.%), H = 0.001 (wt.%), Ti balance. The chemical composition of the alloy was assured by comparing the values specified in the material certificate with the values obtained from atomic emission spectroscopy analysis.

The material was supplied in 100 mm diameter and 1000 mm long rod form. The tensile test and fatigue crack propagation test samples, to be heat-treated, were prepared by cutting 100-mm-diameter and 4-mm-thick pieces by wire erosion. Ti-15V-3Al-3Sn-3Cr alloy was solutionized at 860 °C (above the T_β temperature 740 °C) for 1.5 h and rapidly cooled to room temperature with furnace with argon atmosphere. In the tensile tests, after solution treatment, the tensile strength of the alloy was measured to be 670 MPa, the yield strength was 645 MPa, and the % elongation was 4%.

2.1 Application of Aging Treatments

In the literature, single-step and duplex aging treatments are applied in two different temperature ranges: low temperature (200-450 °C) and high temperature (550-700 °C) (Ref 5, 14). In this study, single-step aging treatment was applied at intervals of 50 °C, including low and high aging treatment temperatures between 300 and 550 °C. Aging treatment time has been determined as 5, 10, 20 and 40 h in order to investigate in detail the mechanical and microstructural properties before and after over-aging, with reference to the studies in the literature (Ref 9, 13).

Duplex aging treatments are applied in two steps: pre-aging treatment and second-step aging treatment. While ω_{iso}/β interfaces are formed during pre-aging treatments, α phases are precipitated on these interfaces in the second-step aging treatments (Ref 14). For this reason, the temperature and times at which these ω_{iso} phases occur most in the pre-aging treatments have been determined by considering the studies in the literature. While selecting pre-aging treatment temperatures and times in duplex aging treatments, 24 h at 250 °C and 10 h at 300 °C were preferred based on previous studies (Ref 9, 18). In the literature, it has been observed that second-step aging treatments are applied in less than 24 h in duplex aging treatments. For this reason, the second-step aging treatment time in duplex aging treatments has been determined as 5, 10 and 20 h. While analyzing the test results of sample groups, a coding system was used to eliminate possible confusion. A detailed description of the coding system and aging treatment temperature and time is given in Table 1.

It is also known that the heating rate in aging treatment directly affects the mechanical properties of metastable β titanium alloys (Ref 11). Studies have shown that low heating rate increases the volume fraction of α phases (Ref 19, 20). For this reason, the sample was heated to aging temperature at a low heating rate of 5 °C/min, held at this temperature for the time of the treatment, and cooled in the furnace environment. All the aging treatment steps were carried out in an argon atmosphere.

2.2 Mechanical Tests

Tensile tests were carried out on samples prepared in accordance with the ASTM E8M standard, loading rate of 1 mm/min, using Instron brand universal tester with 100 kN capacity (Ref 21). Each test was repeated three times, and average results are given in the article. Vickers microhardness measurements were taken under load of 50 g, applying the load for 10 s. Microhardness values were measured from 10 different points and averaged.

Fatigue crack propagation tests samples were prepared in accordance with the ASTM E-647 standard (Ref 22). In order to examine the fatigue crack propagation behavior of the alloy, samples with optimum mechanical properties were selected and fatigue crack propagation tests were applied. Fatigue crack propagation tests were started by entering frequency values as well as maximum and minimum loads. During the tests, USB microscope was used to examine the fatigue crack propagation. The crack length was continuously checked with the microscope from the beginning of the test and the load cycle corresponding to the crack propagation was recorded. The stress intensity factor range was calculated in accordance with the ASTM E-647 standard using Eq 1, where ΔP is the change in load, B is the thickness of the sample, W is the width of the sample, and $\alpha = a/W$ is the ratio of crack length to sample width. The graph of the stress intensity factor range against to crack propagation rate ($da/dN - \Delta K$) was plotted. The material constants C and m were obtained by applying the Paris–Erdogan equation given in Eq 2 to the $da/dN - \Delta K$ curve (Ref 23). The tests were carried out at room temperature, P_{max} = 1500 N, R = 0.1 stress ratio, and 5 Hz frequency. Stress ratios were calculated as given in Eq 3, depending on the minimum and maximum load applied. Threshold stress intensity factor range (ΔK_{th}) value was calculated as ΔK, which corresponds to 10^{-10} m/cycle value of the da/dN value (Ref 22).

$$\Delta K = \frac{\Delta P}{B\sqrt{W}} \left(((2+\alpha))/(1-\alpha)^{(3/2)} \right) \left(0.886 + 4.64\alpha - 13.32\alpha^2 + 14.72\alpha^3 - 5.6\alpha^4\right) \quad \text{(Eq 1)}$$

Table 1 Heat treatment steps, temperature, time and coding designation of the samples groups

Group index	Aging treatment		Coding system
	Temperature, °C	Time	
Solution treatment	860	1.5 h	ST
Single aging treatment	300	5,10, 20 and 40 h	Single aging treatment temperature/time (e.g., 550/20 h)
	350		
	400		
	450		
	550		
Duplex aging treatment			
Pre-aging treatment	250	24 h	250 °C/24 h (I)—second-step aging treatment temperature/time (e.g., I-550/20 h)
	300	10 h	
Second-step aging treatment	450	5, 10 and 20 h	300 °C/10 h (II)—second-step aging treatment temperature/time (e.g., II-550/20 h)
	550		

$$\frac{da}{dN} = C(\Delta K)^m \quad \text{(Eq 2)}$$

$$R = \frac{P_{min}}{P_{max}} \quad \text{(Eq 3)}$$

2.3 Microstructural Investigations

Microstructural analysis and phase transformations were performed using scanning electron microscopy (SEM) and x-ray diffraction techniques. Samples were prepared in accordance with metallographic sample preparation techniques for microstructural investigation, polished with 1 μm alumina solution at the last stage, and 2 mL HF, 2 mL HNO_3 and 100 mL H_2O were used as etching solution. Etching time varied between 15 and 45 s depending on the type of heat treatment applied. Microstructural examinations and the fracture surfaces of the samples after the tensile and fatigue crack propagation tests were analyzed with a LEO 1430 VP model SEM. Phase transformations were studied using a Bruker D8 Advance Model XRD with a 2.2 KW Cu anode with step size 2°/min converting 2θ values in the range of 30°-90°.

3. Results and Discussion

3.1 Microstructural Investigations and XRD Phase Analysis

Ti-15V-3Al-3Sn-3Cr alloy was solution-treated above the T_β temperature at 860 °C for 1.5 h, and the average grain size was determined to be 300 μm. Aging treatment applied at low temperatures slows the diffusion rate of alloying elements and the growth of precipitates decreases. However, the high aging temperature provides a great driving force for intragranular α growth but reduces the precipitation of phases due to relatively low insufficient cooling (Ref 24). Therefore, 300/10 h sample, which was aged at low temperature, was not completed phase transformations, α phases were formed very small in the 300/10 h sample compared to the 550/10 h and large precipitate free zones were formed (Fig. 1a). Due to the increase in aging temperature and the acceleration of aging kinetics, α phases precipitated with high volume fraction on microstructure these zones disappeared completely in the 550/10 h sample (Fig. 1b). Accordingly, α phases in the 300/10 h sample occurred at a lower volume fraction compared to the 550/10 h sample. Aging time as well as aging temperature affects the phase precipitation. In Fig. 1(c), the distribution of the α phases in the samples that have been aged for 40 h at 550 °C is shown. While the α phases are formed in smaller sizes in the sample where the aging treatment is applied for 10 h, with the increase of the aging treatment time to 40 h, the α phases are formed in fine and coarse and non-uniform distribution (Fig. 1c).

It is known that α phases show finer and more uniform distribution in the microstructure of samples that have been duplex aging-treated (Ref 13). With the application of duplex aging treatment, as seen in Fig. 2, α phases are dispersed in the microstructure as finer precipitates. In Fig. 2, microstructural images of the 550/20 h sample with a single-step aging treatment and the I-550/20 h and II-550/20 h samples with duplex aging treatment are shown. In the 550/20 h sample, the coarser α phases occurred (Fig. 2a), while in the I-550/20 h sample, the α phases showed a finer, higher volume fraction and uniform distribution throughout the entire microstructure (Fig. 2b). As can be seen, the pre-aging treatment applied at low temperature provided the formation of metastable phases. In the second-step aging treatment, these metastable phases have enabled the α phases to be formed in finer and high volume fraction. While applying duplex aging treatments, two different pre-aging procedures were chosen: 24 h at 250 °C and 10 h at 300 °C. When the effect of these two different pre-aging procedures on the phase distribution is examined, it can be seen that the α phases are formed more finely when applied the pre-aging 24 h at 250 °C (Fig. 2b). Santhosh et al. explained this situation by the fact that pre-aging process at 250 °C causes more uniformly distributed precursor formation (Ref 9). In the sample, where pre-aging is applied for 10 h at 300 °C, it can be seen that the α phase precipitates are formed in larger sizes due to the increase in the pre-aging temperature (Fig. 2c).

XRD phase analysis shows that the solution-treated sample consisted completely of β phases (Fig. 3a). During single-step aging treatments, the aging temperature and time directly affect the formation of the α phases. In this study, as the aging time increased from 5 to 40 h at 550 °C, there was a significant increase in all the α phase peak intensities. This is an indication that the amount of α phase precipitation increases with increasing aging time. In order to determine the effect of

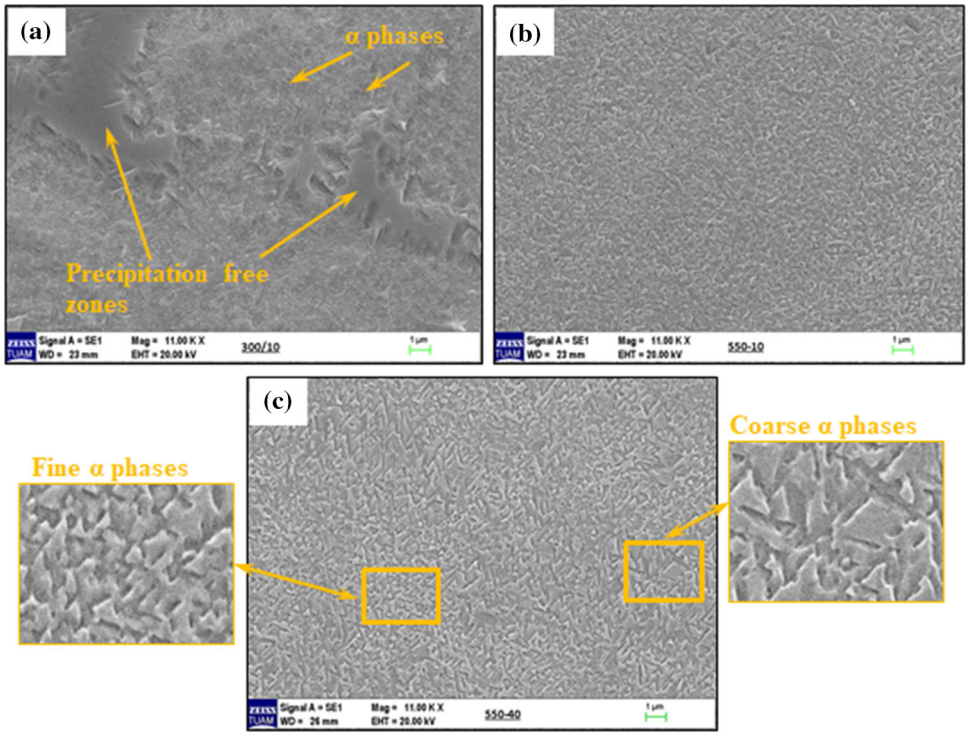

Fig. 1 Microstructure of single-step-aged samples (a) 300/10 h, (b) 550/10 h, (c) 550/40 h

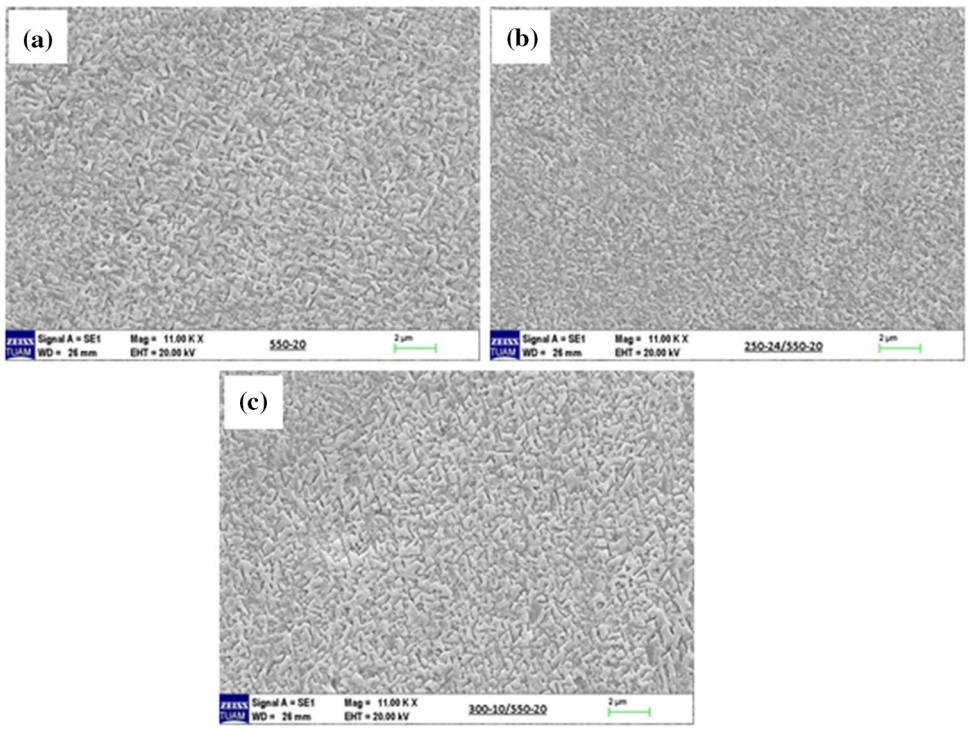

Fig. 2 Microstructure of duplex-aged samples: (a) 550/20 h, (b) I-550/20 h, (c) II-550/20 h

duplex aging treatment on phase transformations, two different pre-aging treatments were applied, and the XRD phase analysis of the samples was examined. In addition, by studying the XRD analyses of 300/10 and 250/24 h samples, phase formations during the pre-aging treatment were determined (Fig. 3b). The metastable ω_{iso} phases were observed in the 300/10 h sample, while the formation of the metastable ω_{iso} phases was not detected in the 250/24 h sample. ω_{iso}/β interfaces are regions where α phases are formed during the second-step aging treatment (Ref 18). Increasing these regions increases the formation of α phase. Therefore, the peak intensities of the α phase were found to be higher in the II-550/20 h sample

compared to the I-550/20 h sample. In particular, the α phase intensity in the α(100) and α(002) line increased significantly and it was observed that the microstructure was mainly composed of α phase in both duplex-aged samples (Fig. 3b).

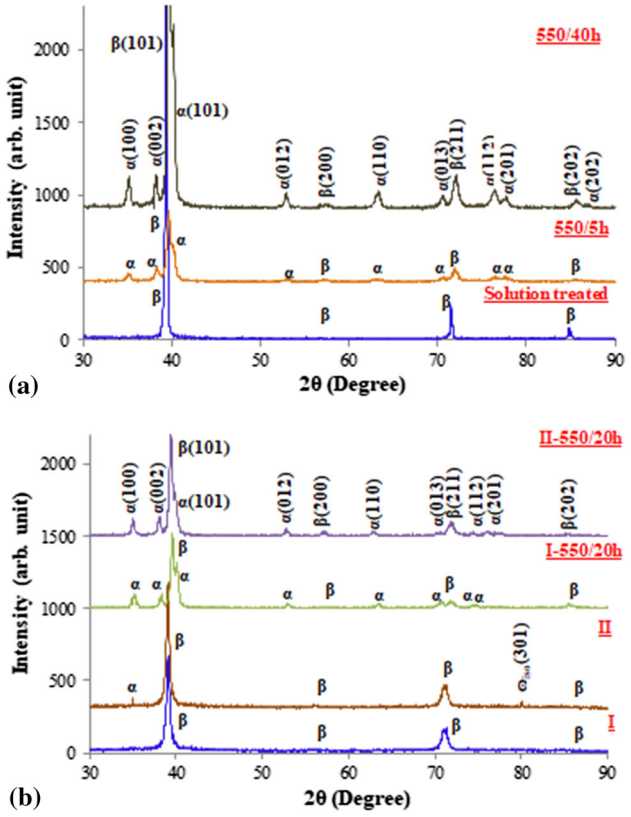

Fig. 3 Results of XRD analysis of aging-treated samples: (a) single-step aging treatment, (b) duplex aging treatment

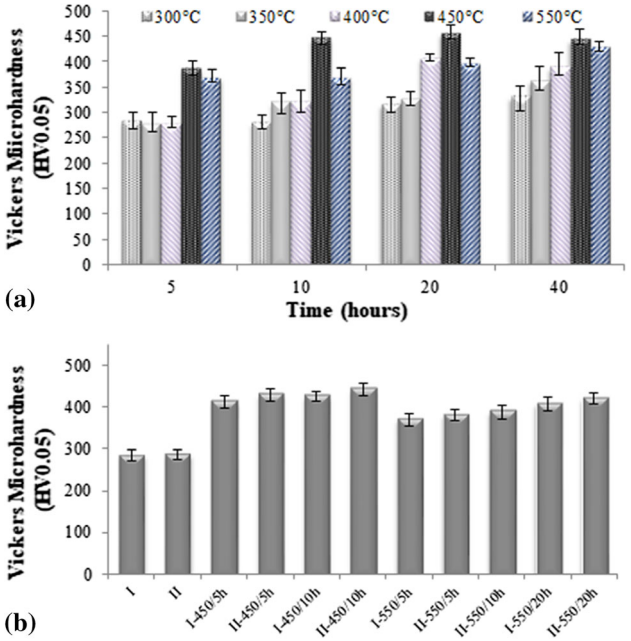

Fig. 4 Microhardness test result of aged samples: (a) single step-aged samples, (b) duplex-aged samples

3.2 Microhardness Test Results

In the aging treatments applied to metastable β titanium alloys, α and ω_{iso} phases precipitate in the β matrix depending on the aging treatment temperature and time. Although the ω_{iso} phases formed at low temperatures increase the microhardness, long periods are required to complete the precipitation (Ref 25). The first significant increase in microhardness occurred at the end of 20 h as a result of the slowing of the aging precipitation at low temperatures, such as 300 and 350 °C. The first significant increase was obtained after 10 h at 400 and 450 °C and 5 h at 550 °C, with the increase of aging temperature (Fig. 4a). In the tests carried out, the maximum microhardness was reached after 450 °C and 20 h, and after this point, the increase in temperature and time caused a decrease in the microhardness. This decrease can be explained by the precipitation and growth of α phases in regions where ω_{iso} phases occur, with increasing aging temperature and time (Ref 13). Microhardness decreased with ω_{iso} phases disappearing as seen in Fig. 4(a).

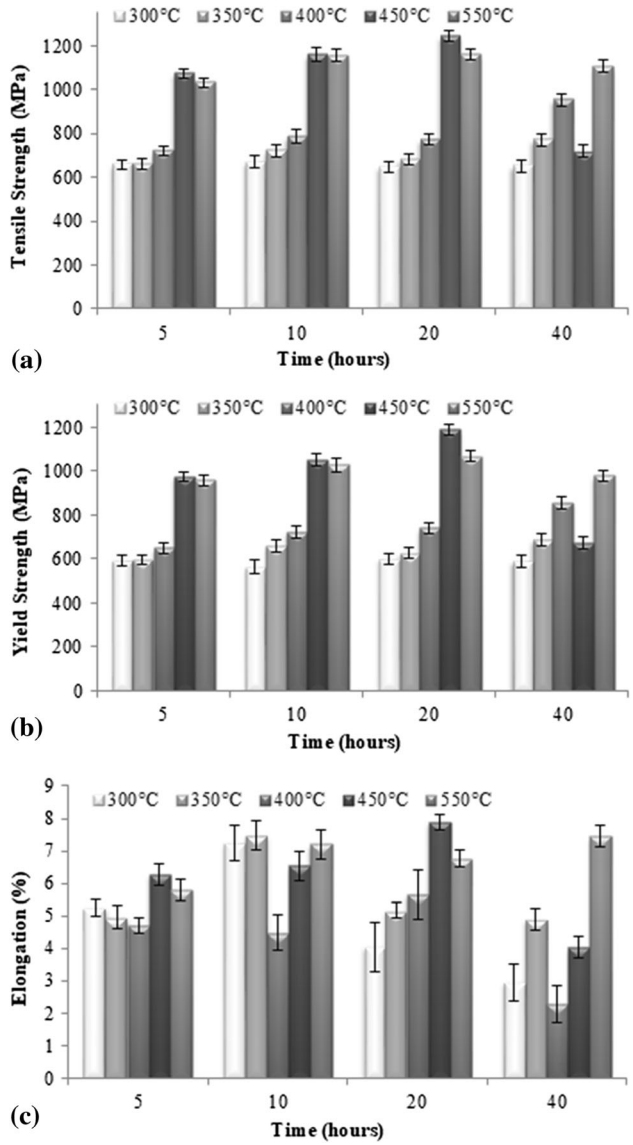

Fig. 5 Single-step aging treatment tensile test results: (a) tensile strength, (b) yield strength, (c) Elongation

While the maximum microhardness value was obtained at 450 °C in duplex aging treatments, the microhardness decreased as the second-step aging treatment temperature increased to 550 °C. Increasing the aging time increased the microhardness in all duplex-aged sample groups. Compared to 250/24 h pre-aging treatment, the 300/10 h pre-aging treatment has a higher microhardness in the samples.

The formation of ω_{iso} phases was observed after the aging treatment of 300/10 h, and these phases caused the α phases to be precipitation intensively during the second-step aging treatments. The α phases, finely and uniformly dispersed in the microstructure, increased the microhardness of the alloy. In the 250/24 h pre-aging treatment, the absence of the ω_{iso} phase formation slowed down the α phase formation in the second-step aging treatments and caused the microhardness to be lower (Fig. 4b).

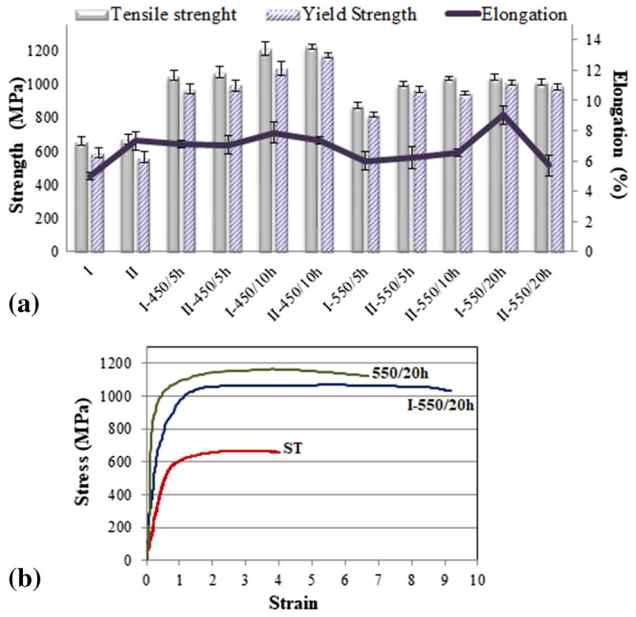

Fig. 6 (a) Tensile test results of duplex aging-treated samples, (b) stress–strain plots of heat-treated samples

3.3 Tensile Test Results

The maximum tensile properties for the each treatment temperature were obtained after 10 h at 300 and 350 °C, and 20 h at 400, 450, and 550 °C (Fig. 5). Phase transformations could not be completed due to the slow precipitation kinetics at low aging temperatures of 300 and 350 °C. Therefore, there was no significant increase in tensile strength, yield strength and % elongation at these two temperatures. The maximum tensile properties were obtained after aging for 10 h, after which the increase in time caused a small increase in the tensile and yield strength of the alloy, while the % elongation was significantly reduced. This can be explained by the ω_{iso} phases formed in the microstructure in this temperature range. While the ω_{iso} phases occur rapidly at low temperatures, their growth is realized by moving β elements from the ω_{iso} phases to the matrix, depending on the time. Although the ω_{iso} phases formed in this way at long aging times increases its tensile and yield strength, it decreases the % elongation of the alloy by causing a shortening of the sliding bands in the β matrix. However, in the early stages of the ω_{iso} phase precipitation, it increases the tensile and yield strength of metastable β titanium alloys without reduction of % elongation (Ref 25). As seen in Fig. 5, when the time was increased to 20 and 40 h, the ω_{iso} phases caused a small increase in tensile and yield strength values while reducing the % elongation. With the aging temperature increasing to 400 and 450 °C, the increase in

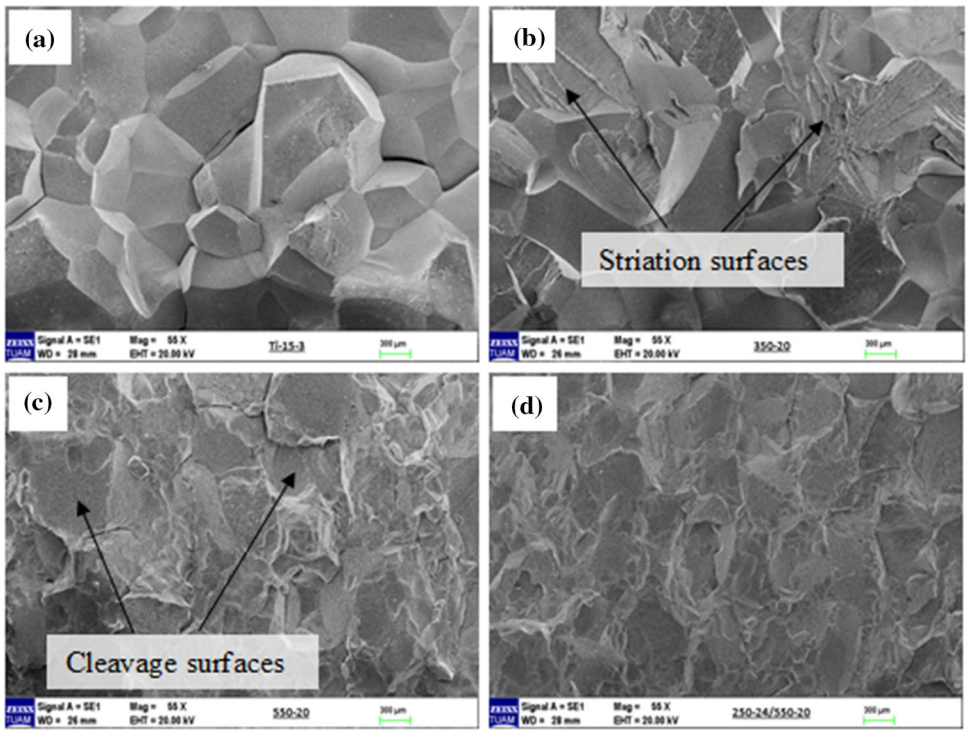

Fig. 7 Fracture surfaces of aging-treated samples, (a) solution-treated sample, (b) 350/20 h, (c) 550/20 h, (d) I-550/20 h

tensile and yield strength becomes evident. Fine and uniform dispersed α phases formed in the microstructure serve as a barrier to prevent dislocations during deformation. The α phases formed in this way increased the tensile strength of the alloy by 100% after 5 h at 450 °C. During the first 20 h at 450 °C aging temperatures, the tensile and yield strength and % elongation of the alloy continuously increased. At 550 °C, which is a high aging temperature, the effect of the aging treatment on the tensile and yield strength and % elongation was obvious, even after 5 h. At this temperature, the increase in tensile and yield strength and % elongation continued up to 20 h, and then the % elongation increased with the growth of α phases, while the tensile and yield strength decreased.

In duplex aging treatments, the aim is to produce a fine and uniform precipitation of the α phases and to reduce the precipitation-free zones which have a detrimental effect on the mechanical properties. ω_{iso} metastable phases, which occur in the microstructure with the pre-aging treatment, affect the α phase precipitation behavior depending on the aging treatment temperature and time applied in the second step (Ref 18). The finely precipitated α phases are uniformly dispersed throughout the microstructure, so that the precipitation-free zones are eliminated, and the tensile strength and yield strength of the alloy are increased. Also, the gradual application of the duplex aging treatment, as a pre-aging and second-step aging treatment, limits the formation of grain boundary alpha (α_{GB}) phases. For this reason, the % elongation of these samples is higher compared to the samples with a single-step aging treatment. After both pre-aging treatments, a second-step aging treatment was applied at 450 and 550 °C (Fig. 6a). Optimum tensile properties were obtained in the duplex-aged sample, which was aged at 550 °C for 20 h after pre-aged at 250 °C for 24 h. The stress–strain plots of I-550/20, 550/20 h and solution-treated samples are given in Fig. 6(b). When the stress–strain plots are compared, it is seen that with the duplex aging treatment higher % elongation with without sacrificing tensile strength is obtained compared to the single-step aging-treated sample.

In the solution-treated sample, intergranular fracture occurred, and brittle damaged surface was observed (Fig. 7a). Similarly, brittle fracture behavior was also observed in samples that were aged at low temperatures. Wide cleavage surfaces and striations occurred in the sample which was aged at 350 °C (Fig. 7b). This situation occurs when the ω_{iso} phases limit the formation of shear systems and lead to planar shifts of dislocations (Ref 26). In the 550/20 h sample, the effects of increasing the aging temperature on the damage surfaces of the sample can be seen. The ductility due to the increase of the aging temperature caused the sample's fracture type to change from intergranular to transgranular. In the 550/20 h sample, the fracture surfaces are predominantly composed of transgranular and dimple structures, with partially observed flat cleavage surfaces (Fig. 7c). In the I-550/20 h sample reduced particle separation and the sample showed more ductile fracture behavior. Also, dimple structures and cleavage fractures were observed on the fracture surface (Fig. 7d).

3.4 Effect of Aging Treatment on Fatigue Crack Propagation Behavior

Fatigue crack propagation tests were carried out on the samples where solution treatment, single-step and duplex aging treatments were applied. Fatigue crack propagation progressed along the grain boundaries in the solution-treated samples. In the samples with aging treatment, fatigue crack propagation proceeded non-crystallographically in the grains with α phase formations. In this group of samples, the crack propagated through the α phases in the matrix.

In aging-treated samples where fine uniform α phases are formed, the cracks propagated by following small spacing between the α phases. Therefore, compared to the solution-treated sample, the total crack length has been shortened and the fatigue crack propagation rate has increased (Fig. 8a). For this reason, the fine and high-volume-fraction α phases that

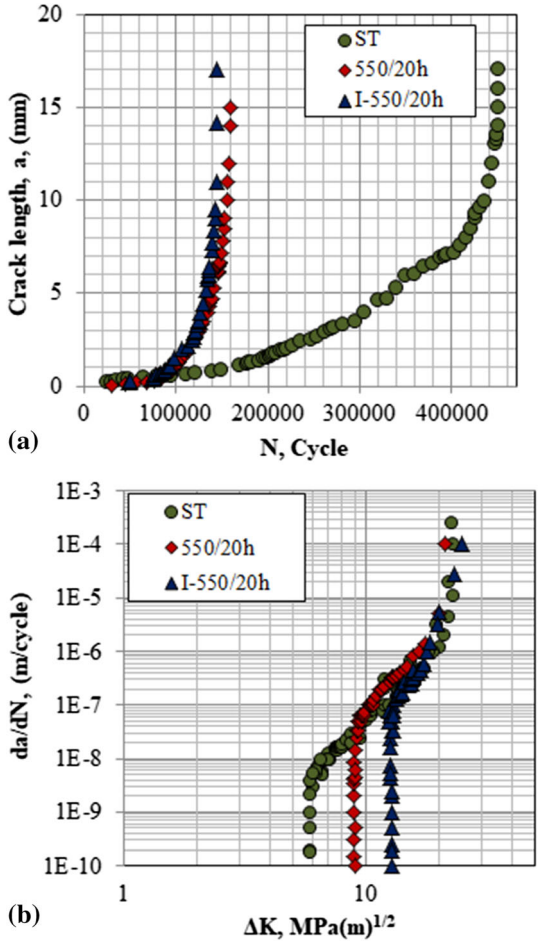

Fig. 8 The effect of aging treatment on fatigue crack propagation rate of Ti-15V-3Al-3Sn-3Cr metastable β titanium alloy (a) a-N, (b) $da/dN - \Delta K$

Table 2 Threshold stress intensity factor range (ΔK_{th}), C and m material constants of solution-treated and aging-treated samples

Sample	m	C	ΔK_{th}
Solution treated	3.5	8E−09	5.9
550/20 h	5.62	2E−13	9
I-550/20 h	6.93	2E−15	12.9

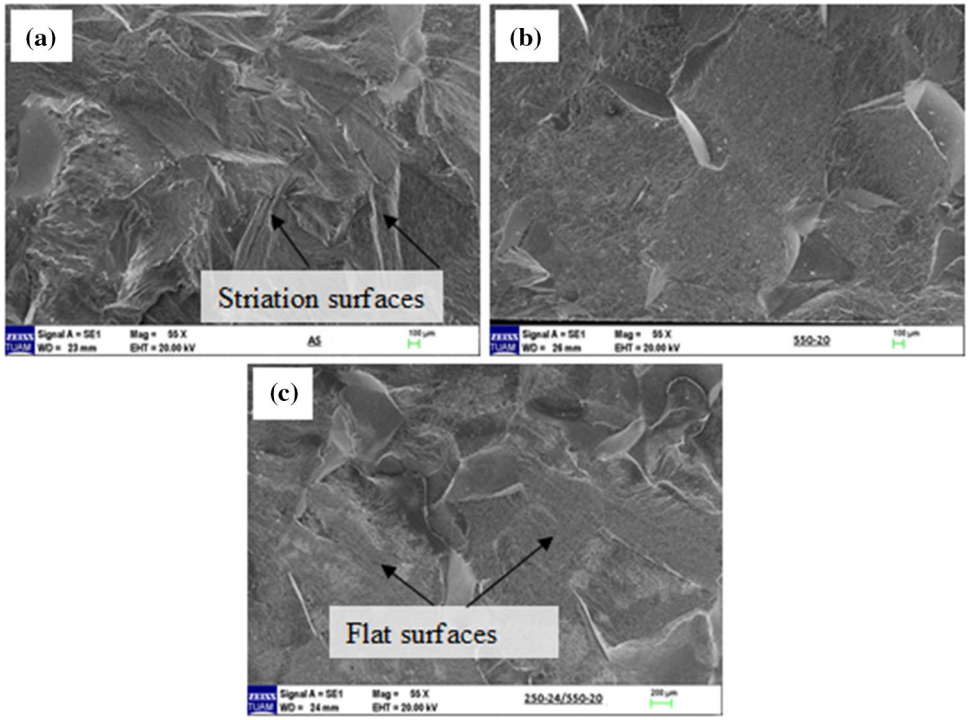

Fig. 9 Fracture surfaces of fatigue crack propagation test samples, (a) solution-treated sample, (b) 550/20 h, (c) I-550/20 h

increase the mechanical properties of the alloy have increased the fatigue crack propagation rate. Another result obtained in the fatigue crack propagation tests was that the fatigue crack growth was delayed and the ΔK_{th} values were higher in the alloy with the aging treatment (Fig. 8b).

Material constants and ΔK_{th} values obtained in the fatigue crack propagation tests are given in Table 2. Due to the occurrence of the high volume fraction of fine α phases in the duplex aging treatments, the highest ΔK_{th} value and the highest crack propagation rate were obtained in the I-550/20 h sample.

It can be seen that the fracture surface consists of striation structures in the solution-treated sample (Fig. 9a). As the fatigue crack propagates along the grain boundaries, a striation damaged surface has been formed within each grain. Previous studies have reported that the striation damaged surfaces occur during cyclical loading (Ref 10). The fracture surface has a high roughness in this sample and consists of cleavage surfaces in some regions. With the application of the aging treatment, the striation structures on the surface decreased and the surface became smoother in the 550/20 h and I-550/20 h samples (Fig. 9b and c).

4. Conclusions

The effect of single-step and duplex aging treatments on the microstructural properties, tensile properties and fatigue crack growth and propagation behavior of the Ti-15V-3Al-3Sn-3Cr metastable β titanium alloy was investigated. The results obtained in the study are listed below.

- 300/10 h pre-aging treatment increased the precipitation of α phases compared to the 250/24 h pre-aging treatment. Depending on this situation, microhardness was found to be higher in the samples with 300/10 h pre-aging treatment.
- Optimum mechanical properties were obtained in the duplex-aged samples, which was aged at 550 °C for 20 h after pre-aged at 250 °C for 24 h.
- The fine, high volume fraction and uniformly dispersed α phases increased the tensile strength and % elongation of the alloy in the duplex aging treatment, but also increased the fatigue crack propagation rate.
- Fatigue crack growth resistance was increased with the application of aging treatment, and the highest ΔK_{th} value was obtained in the sample to which duplex aging treatment was applied depending on precipitation of fine and high volume fraction of α phases.

Acknowledgments

The authors gratefully acknowledge Afyon Kocatepe University Scientific Research Projects Commission for the financial support Project number: 18.FEN.BİL.62.

References

1. P. Singh, H. Pungotra, and N.S. Kalsi, On the Characteristics of Titanium Alloys for the Aircraft Applications, *Mater. Today Proc.*, 2017, **4**, p 8971–8982
2. J.D. Cotton, R.D. Briggs, R.R. Boyer, S. Tamirisakandala, P. Russo, N. Shchetnikov, and J.C. Fanning, State of the Art in Beta Titanium

Alloys for Airframe Applications, *JOM Min. Met. Mater. Soc.*, 2015, **67**, p 1281–1303. https://doi.org/10.1007/s11837-015-1442-4
3. F.H. Froes and H.B. Bomberger, The Beta Titanium Alloys, *JOM*, 1985, **37**(7), p 28–37
4. R. Kolli and A. Devaraj, A Review of Metastable Beta Titanium Alloys, *Metals (Basel)*, 2018, **8**(7), p 506. https://doi.org/10.3390/met8070506
5. G. Qiang, W. Qing, S. Dong-Li, H. Xiu-Li, and W. Gao-Hui, Formation of Nanostructure and Mechanical Properties of Cold-Rolled Ti–15V–3Sn–3Al–3Cr Alloy, *Mater. Sci. Eng., A*, 2010, **527**(16–17), p 4229–4232 ((In English))
6. H. Fujii and H.G. Suzuki, Effect of Solutioning Conditions on Aging Response in Ti–15V–3Cr–3Sn–3Al, *Mater. Trans.*, 1993, **34**(4), p 373–381 (in English)
7. T.W. Xu, H.C. Kou, J.S. Li, F.S. Zhang, and Y. Feng, Effect of Phase Transformation Conditions on the Microstructure and Tensile Properties of Ti-3Al-15Mo-3Nb-0.2Si Alloy, *J. Mater. Eng. Perform.*, 2015, **24**(8), p 3018–3025
8. C.L. Li, X.J. Mi, W.J. Ye, S.X. Hui, Y. Yu, and W.Q. Wang, A Study on the Microstructures and Tensile Properties of New Beta High Strength Titanium Alloy, *J. Alloys Compd.*, 2013, **550**, p 23–30 (in English)
9. R. Santhosh, M. Geetha, V.K. Saxena, and M. Nageswararao, Studies on Single and Duplex Aging of Metastable Beta Titanium Alloy Ti-15V-3Cr-3Al-3Sn, *J. Alloys Compd.*, 2014, **605**, p 222–229
10. P. Schmidt, A. El-Chaikh, and H.J. Christ, Effect of Duplex Aging on the Initiation and Propagation of Fatigue Cracks in the Solute-Rich Metastable β Titanium Alloy Ti 38-644, *Metall. Mater. Trans. A*, 2011, **42**(9), p 2652–2667 (in English)
11. A.S. Arcelormittal, M. Dehmas, A. Settefrati, G. Geandier, B. Denand, E. Aeby-Gautier, B. Appolaire, G. Khelifati, and J. Delfosse, *Precipitation Sequences in Beta Metastable Phase of Ti-5553 Alloy during Ageing. Ti-2011*, Science Press Beijing, Beijing, 2011, p 468–472 (In English)
12. S. Ankem and S.R. Seagle, Heat treatment of Metastable Beta Titanium Alloys, *Beta Titanium Alloys in the 1980′s*, R.R. Boyer and H.W. Rosenberg, Ed., The Metallurgical Society of AIME, Englewood, 1984, p 107–126 (In English)
13. R. Santhosh, M. Geetha, V.K. Saxena, and M. NageswaraRao, Effect of Duplex Aging on Microstructure and Mechanical Behavior of Beta Titanium Alloy Ti-15V-3Cr-3Al-3Sn under Unidirectional and Cyclic Loading Conditions, *Int. J. Fatigue*, 2015, **73**, p 88–97
14. T. Furuhara, T. Maki, and T. Makino, Microstructure Control by Thermomechanical Processing in b-Ti-15-3 Alloy, *J. Mater. Process. Technol.*, 2001, **117**(3), p 318–323 (in English)
15. Y.K. Chou, L.W. Tsay, and C. Chen, Effects of Aging Treatments on the Mechanical Behavior of Ti-15V-3Cr-3Sn-3Al Alloy, *J. Mater. Eng. Perform.*, 2015, **24**(9), p 3365–3372
16. R.R. Boyer, An Overview on the Use of Titanium in the Aerospace Industry, *Mater. Sci. Eng., A*, 1996, **213**, p 103–114 (in English)
17. S.S.J. Li, T.C. Cui, Y.L. Hao, and R. Yang, Fatigue Properties of a Metastable [Beta]-Type Titanium Alloy with Reversible Phase Transformation, *Acta Biomater.*, 2008, **4**(2), p 305–317 (in English)
18. T. Furuhara, S. Takagi, H. Watanabe, and T. Maki, Crystallography of Grain Boundary α Precipitates in a β Titanium Alloy, *Metall. Mater. Trans. A Phys. Metall. Mater. Sci.*, 1996, **27**(6), p 1635–1646
19. N. Wain, X.J. Hao, G.A. Ravi, and X. Wu, The Influence of Carbon on Precipitation of α in Ti-5Al-5Mo-5V-3Cr, *Mater. Sci. Eng., A*, 2010, **527**(29–30), p 7673–7683
20. Q. Contrepois, M. Carton, and J. Lecomte-Beckers, Characterization of the β Phase Decomposition in Ti-5Al-5Mo-5V-3Cr at Slow Heating Rates. *Open J. Met.* (2011). http://www.scirp.org/journal/ojmetal. Accessed 14 July 2020
21. American Society for Testing and Materials, *ASTM E8 M: Standard Test Methods for Tension Testing of Metallic Materials*, American Society for Testing and Materials, Philadelphia, 2000
22. American Society for Testing and Materials, *ASTM E647: Standard Test Method for Measurement of Fatigue Crack Growth Rates*, American Society for Testing and Materials, Philadelphia, 2008
23. P. Paris and F. Erdogan, A Critical Analysis of Crack Propagation Laws, *J. Basic Eng.*, 1963, **85**(4), p 528–533
24. H.Y. Zhang, Z.P. Zhang, Z.Y. Li, J. Sun, X. Che, S.Q. Zhang, Y. Liang, and L.J. Chen, Low-Cycle Fatigue Behavior of Ti-6Mo-5V-3Al-2Fe Alloy with Various Types of Secondary α Phase, *Mater. Res. Express*, 2020, **7**(2), p 26555. https://doi.org/10.1088/2053-1591/ab756a
25. F. Prima, P. Vermaut, D. Ansel, and J. Debuigne, ω Precipitation in a Beta Metastable Titanium Alloy, Resistometric Study, *Mater. Trans.*, 2001, **41**(8), p 1092–1097 (in English)
26. W.F. Cui and A.H. Guo, Microstructures and Properties of Biomedical TiNbZrFe β-Titanium Alloy under Aging Conditions, *Mater. Sci. Eng., A*, 2009, **527**(1–2), p 258–262